

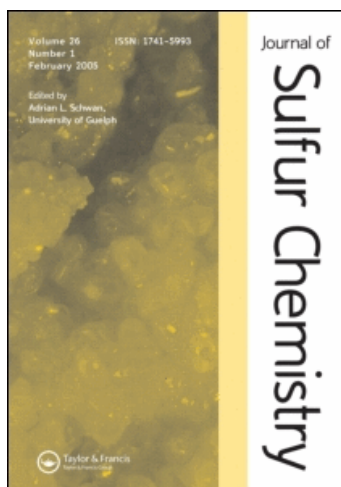
This article was downloaded by:

On: 25 January 2011

Access details: *Access Details: Free Access*

Publisher *Taylor & Francis*

Informa Ltd Registered in England and Wales Registered Number: 1072954 Registered office: Mortimer House, 37-41 Mortimer Street, London W1T 3JH, UK



Journal of Sulfur Chemistry

Publication details, including instructions for authors and subscription information:

<http://www.informaworld.com/smpp/title~content=t713926081>

An estimate of the equilibrium speciation of sulfur vapor over solid sulfur and implications for planetary atmospheres

James R. Lyons^a

^a Department of Earth and Space Sciences, Institute of Geophysics and Planetary Physics, University of California, Los Angeles, CA, USA

To cite this Article Lyons, James R.(2008) 'An estimate of the equilibrium speciation of sulfur vapor over solid sulfur and implications for planetary atmospheres', *Journal of Sulfur Chemistry*, 29: 3, 269 – 279

To link to this Article: DOI: 10.1080/17415990802195615

URL: <http://dx.doi.org/10.1080/17415990802195615>

PLEASE SCROLL DOWN FOR ARTICLE

Full terms and conditions of use: <http://www.informaworld.com/terms-and-conditions-of-access.pdf>

This article may be used for research, teaching and private study purposes. Any substantial or systematic reproduction, re-distribution, re-selling, loan or sub-licensing, systematic supply or distribution in any form to anyone is expressly forbidden.

The publisher does not give any warranty express or implied or make any representation that the contents will be complete or accurate or up to date. The accuracy of any instructions, formulae and drug doses should be independently verified with primary sources. The publisher shall not be liable for any loss, actions, claims, proceedings, demand or costs or damages whatsoever or howsoever caused arising directly or indirectly in connection with or arising out of the use of this material.

An estimate of the equilibrium speciation of sulfur vapor over solid sulfur and implications for planetary atmospheres

James R. Lyons*

Department of Earth and Space Sciences, Institute of Geophysics and Planetary Physics, University of California, Los Angeles, CA, USA

(Received 27 January 2008; final version received 12 May 2008)

Sulfur allotropes have been observed in planetary atmospheres and are believed to have been present in the ancient Earth atmosphere. The vapor pressures of sulfur allotropes, especially S_2 , S_3 , and S_4 , are poorly known at typical atmospheric temperatures, but have generally been assumed to be high enough to represent significant gas phase abundances in model calculations. Here I present estimates of the speciation of the equilibrium vapor pressure over solid sulfur, which would seem to imply that the vapor pressures of most allotropes are too low at typical atmospheric temperatures for gas phase formation reactions to be important. However, consideration of the kinetics of condensation shows that gas phase sulfur allotrope reactions can be important under certain conditions. The implications for the mechanism of sulfur isotope mass-independent fractionation on early Earth are discussed. Implications for the presence of sulfur allotropes in Venusian clouds, the distribution of S_2 in the atmosphere of Jupiter following the comet Shoemaker-Levy 9 impacts, and the observation of S_2 in volcanic plumes on Io are also presented.

Keywords: sulfur allotropes; vapor pressure; atmospheric chemistry; mass-independent fractionation; planetary atmospheres

1. Introduction

Sulfur allotropes, particularly S_2 , S_4 , and S_8 , have been predicted to be important gas phase species in the ancient, low O_2 Earth atmosphere (1–3). The recent discovery (4) of sulfur isotope mass-independent fractionation (S-MIF) in ancient rocks (>2.4 Gyr in age) has further raised the prospect of gas phase sulfur allotrope reactions in the atmosphere. This discovery promises to yield both qualitative and quantitative insights into the composition of the paleoatmosphere, but the mechanism responsible for the S-MIF is still debated.

Although I will not discuss the S-MIF signatures in detail here, it will be helpful to define mass-independent fractionation (MIF). The origin of mass-dependent fractionation (MDF) in isotope systems lies in the mass dependence of the molecular properties (*e.g.* zero-point energy) and physical processes (*e.g.* evaporation) affecting the compound. Mass-dependent processes

*Email: jimlyons@ucla.edu

yield isotopic fractionations of the rare isotopes (normalized to the most abundant isotope, *i.e.* $^{17}\text{O}/^{16}\text{O}$ and $^{18}\text{O}/^{16}\text{O}$ for oxygen isotopes) that are proportional to the mass differences (1 amu for ^{17}O and 2 amu for ^{18}O), and so are related by a factor of approximately 0.5. If a compound with three or more stable isotopes, such as oxygen or sulfur, deviates from a mass-dependent relationship, the compound is said to exhibit non-MDF or MIF. MIF signatures are not affected by mass-dependent processes (*e.g.* evaporation, kinetic isotope effects, zero-point differences, etc.), and so are excellent tracers of the small number of mass-independent processes that exist in nature. Examples of MIF processes include self-shielding during photodissociation of molecules with line-type spectra, and non-statistical effects that occur during vibrational de-excitation.

MIF in oxygen isotopes (O-MIF) is well known in primitive meteorites (5) and in atmospheric O_3 (6). In terrestrial environments, O-MIF is present in many atmospheric molecules and aeolian sediments, and is nearly always a result of interactions with atmospheric ozone. It is believed that MIF in O_3 results from the non-statistical randomization of energy in vibrationally excited O_3 during the O_3 formation reaction, $\text{O} + \text{O}_2 \xrightarrow{\text{M}} \text{O}_3$, in a manner that depends on the symmetry of the O_3 isotopomer (7). (M is a third body molecule such as N_2 that serves to stabilize the vibrationally excited complex.) The source of O-MIF in primitive meteorites is unknown but has been attributed to self-shielding during photodissociation of CO in the solar nebula (8–10), and also to ozone-like non-statistical reactions on mineral grain surfaces (11), a hypothesis not yet verified in the laboratory. By analogy with the formation of oxygen MIF during gas phase O_3 formation, it is possible that the isoelectronic reaction, $\text{S} + \text{S}_2 \xrightarrow{\text{M}} \text{S}_3$, is a source of S-MIF in the early Earth atmosphere. Although the vapor pressures for S_2 and S_4 are not specified in atmospheric models (1), the vapor pressure of total sulfur vapor over solid sulfur appears to be highly supersaturated, especially if extrapolated to typical atmospheric temperatures of less than 300 K. Self-shielding during SO_2 photolysis has also been proposed to be the source of S-MIF on early Earth (12).

In addition to predictions for the primitive Earth atmosphere, sulfur allotropes have also been detected or inferred to be present in planetary atmospheres. Sulfur allotropes are believed to be present in the atmosphere of Venus. Photolysis of SO_2 in the presence of low concentrations of water vapor yields both H_2SO_4 and elemental sulfur aerosols, which descend into the lower atmosphere and are converted to OCS at high temperatures (13). S_3 and S_4 have been proposed to be the blue absorber that gives the Venus atmosphere its slightly yellowish colour (14). S_2 was observed at one of the impact sites of comet Shoemaker-Levy 9 with Jupiter (15, 16). Photochemical modeling (17) concludes that S_2 was rapidly converted to S_8 during the association reactions. Finally, S_2 absorption features in the B–X band have also been observed in volcanic plumes on Io, the magmatically active moon of Jupiter (18). The plumes emanate from magmatic hot spots on the surface of Io at silicate magma temperatures of ~ 1300 K. In principle, S_2 vapor pressure could be used to infer plume temperature.

Using the published experimental and computed vapor pressures for allotrope vapor pressures over liquid sulfur and for total vapor pressure over solid sulfur, I present estimates of vapor pressure speciation over solid sulfur. These estimates will help to constrain the abundances of sulfur allotropes in the atmospheres of ancient Earth and other planets.

2. Vapor pressure of sulfur allotropes over liquid sulfur

The literature on sulfur vapor pressure over solid and liquid sulfur is replete with errors, often times due to incorrectly accounting for changes in units from earlier publications. Recent work

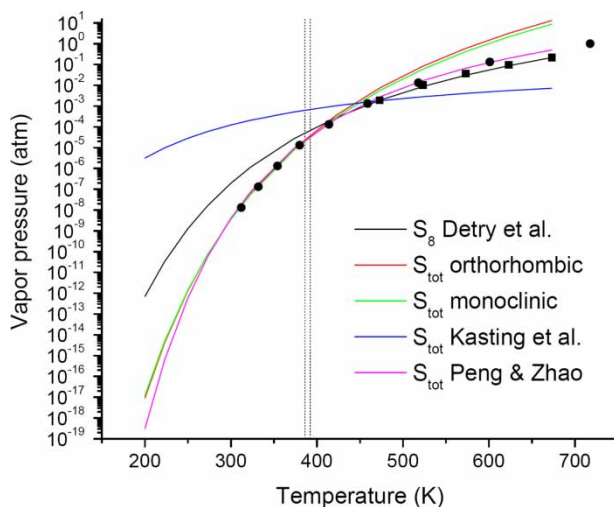


Figure 1. Several published measurements and fits for total sulfur vapor pressure versus temperature. Measured values for total sulfur vapor pressure are shown as filled circles (40). The measured values for S_8 (filled squares) and the fit curve (black) are for liquid sulfur (23). The orthorhombic (red) and monoclinic (green) curves (19) are valid below the appropriate sulfur phase melting point. The Kasting *et al.* curve (blue) is from ref. (1). The Peng & Zhao curve (magenta) is based on a fit to the Wagner Equation (19). The vertical dotted lines indicate the melting points of pure monoclinic (392 K) and orthorhombic (386 K) sulfur (41). Coefficients for vapor pressure fit equations over solid sulfur are given in Table 1.

(19) discusses this and presents corrected total vapor pressure curves. Figure 1 shows several vapor pressure curves for liquid and solid sulfur. The orthorhombic (red) and monoclinic curves (green) are from earlier work (20, 21) and are applicable at temperatures below the sulfur melting point. The vapor pressure of S_8 over liquid sulfur is also shown (black) (22) with the previously published data (23). I have extended the fit to the S_8 vapor pressure to temperatures below the sulfur melting point. Two other curves are given in Figure 1: the vapor pressure curve from Kasting *et al.* (1) and a vapor pressure fit to the Wagner Equation (19). The Kasting *et al.* (1) curve differs greatly from the other curves, especially at low temperatures, possibly due to a typographical error in their vapor pressure equation. In their atmospheric model, Kasting *et al.* (1) assumed that S_8 condensed immediately after formation, which would minimize the significance of the vapor pressure error even if the incorrect equation was used in their model. The Wagner equation vapor pressure curve (19) is shown, because it yields a fairly good fit both above and below the sulfur melting point.

The equilibrium speciation of sulfur vapor over liquid sulfur was investigated by Rau *et al.* (22). They computed equilibrium constants for the set of reactions

$$S_i = \frac{1}{2}iS_2 \quad (1)$$

for $i = 2$ to 8, including real gas corrections. Partial pressures and densities were computed for each S_i , and computed densities were compared with measured densities. The latter was necessary due to uncertainties in thermodynamic data. The agreement between computed (22) and measured (23) partial pressures from 473 to 673 K at 1 atm pressure is quite good. I have fit the measured partial pressures over this temperature range to an expression of the form

$$\log_{10}(p_i) = a_{1,i} - \frac{a_{2,i}}{T}, \quad (2)$$

Table 1. Fit parameters for sulfur vapor pressure^a speciation over liquid and solid sulfur.

| Vapor species | a_1 (atmospheres) | a_2 (K) | Temperature range (K) |
|--------------------------------|---------------------|-----------|-----------------------|
| Total over orthorhombic sulfur | 8.7832 | 5166 | <386 |
| Total over monoclinic sulfur | 8.4832 | 5082 | <392 |
| S_2^b | 7.0240 | 6091.2 | >392 ^b |
| S_3 | 6.3428 | 6202.2 | |
| S_4 | 6.0028 | 6047.5 | |
| S_5 | 5.1609 | 4714.8 | |
| S_6 | 4.8039 | 3814.1 | |
| S_7 | 5.2127 | 4113.6 | |
| S_8 | 4.1879 | 3269.1 | |

^aThe vapor pressure is given by Equation (2) in the text in units of atmospheres; ^bthe vapor pressures for S_2 through S_8 are over liquid sulfur and are applicable to temperatures >392 K.

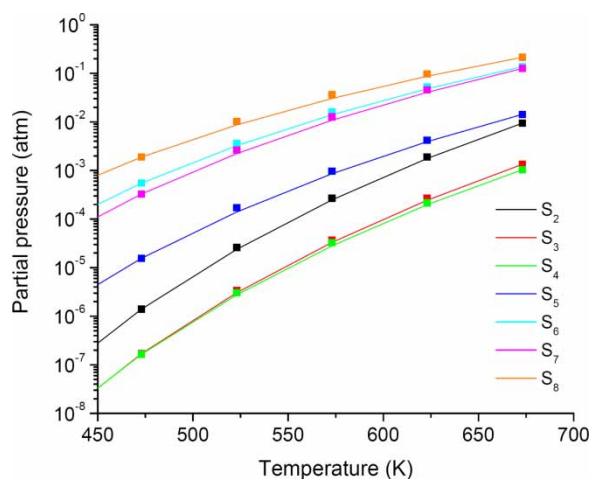


Figure 2. Fits to experimental equilibrium vapor pressure curves for sulfur allotropes over liquid sulfur (22, 23). Fit equation coefficients are given in Table 1. Sulfur allotrope data points are from Detry *et al.* (23) (also listed in Rau *et al.* (22)).

where the fit values are given in Table 1 with p_i in atmospheres and T in K. Figure 2 shows the vapor pressure data (23) and the curves given by Equation (2). As expected S_8 , followed by S_6 and S_7 , has the highest vapor pressure over the temperature range considered. The lowest vapor pressures are obtained for S_2 , S_3 , and S_4 .

Earlier flash photolysis experiments (24, 25) are consistent with the vapor pressures in Figure 2. The experiments were performed on sulfur vapor at ~ 420 – 450 K in which the vapor (primarily S_8) was photolyzed at UV wavelengths. S_2 was observed spectroscopically as a photodissociation product of S_8 . Subsequent loss of the S_2 vapor occurred on timescales $\sim 10^{-5}$ s, and was assumed to be due to 3-body formation of S_4 and S_8 by the gas phase reactions



In the experiments, the predominance of S_8 in the initial vapor and the loss of S_2 after photodissociation of the vapor are expected.

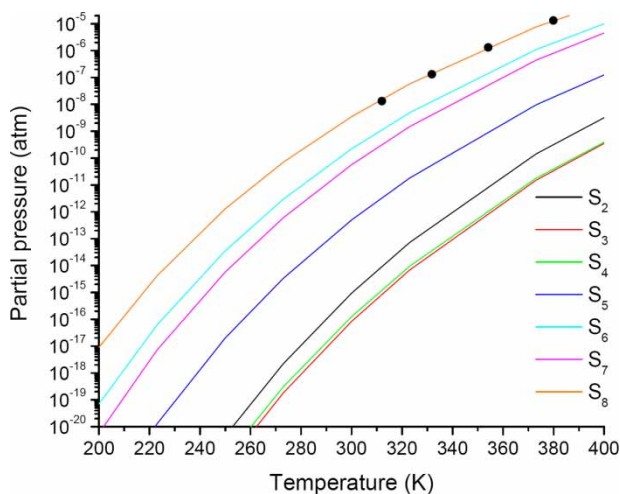


Figure 3. Vapor pressure of sulfur allotropes at temperatures over solid sulfur. Vapor pressure curves are computed by scaling the results in Figure 2 by the ratio of the saturated vapor over solid sulfur to the saturated vapor pressure over liquid sulfur from Detry *et al.* (23) (Figure 1), using Equation (4) as described in the text. Filled circles are measured total sulfur vapor pressure (40).

3. Vapor pressure of sulfur allotropes over solid sulfur

Extrapolation of the vapor pressures in Figure 2 to temperatures below the sulfur melting point would clearly yield erroneous results, as evidenced by the S_8 vapor pressure curve in Figure 1. A better estimate for the low temperature vapor pressures is given by the expression

$$p_i^{\text{sol}}(T) = p_i^{\text{liq}}(T) \frac{p_{\text{sat}}^{\text{sol}}(T)}{p_{\text{sat}}^{\text{liq}}(T)}, \quad (4)$$

where $p_{\text{sat}}^{\text{liq}}(T) = \sum_{i=2}^8 p_i^{\text{liq}}(T)$ is the sum of the vapor pressures as computed in Figure 2, but at a temperature $T <$ the melting point. This approximation assumes that the relative abundances of allotrope vapor pressures at temperatures below the melting point are well approximated by the equations used for temperatures above the melting point (*i.e.* from ref. (22)), even though the absolute vapor pressures over solid are incorrect. The fairly good agreement between measured total vapor pressure and the Wagner equation (Peng & Zhao curve, Figure 1) lends some credibility to this approach. The resulting estimated vapor pressures are shown in Figure 3 for a range of temperatures relevant to most atmospheres.

A typical temperature and pressure profile for the modern Earth atmosphere is shown in Figure 4a. An ancient Earth atmosphere without an ozone layer would likely not have a significant temperature rise in the upper stratosphere, unless some other strong absorber was present. Assuming that the sulfur vapor speciation over liquid does not change significantly with background gas pressure, the resulting vapor pressures curves for Figure 4a are shown in Figure 4b. For a surface temperature of 288 K, the vapor pressures of S_3 and S_4 are $\sim 10^{-17}$ atm and $S_2 \sim 10^{-16}$ atm, corresponding to number densities $\sim 10^2$ to 10^3 cm^{-3} (these values are about an order of magnitude higher than estimates I recently reported (12)). Corresponding profiles for the atmosphere of Venus (26), which are given in Figure 5a and b illustrate the low vapor pressures expected for sulfur allotropes at Venus cloud heights (40–60 km).

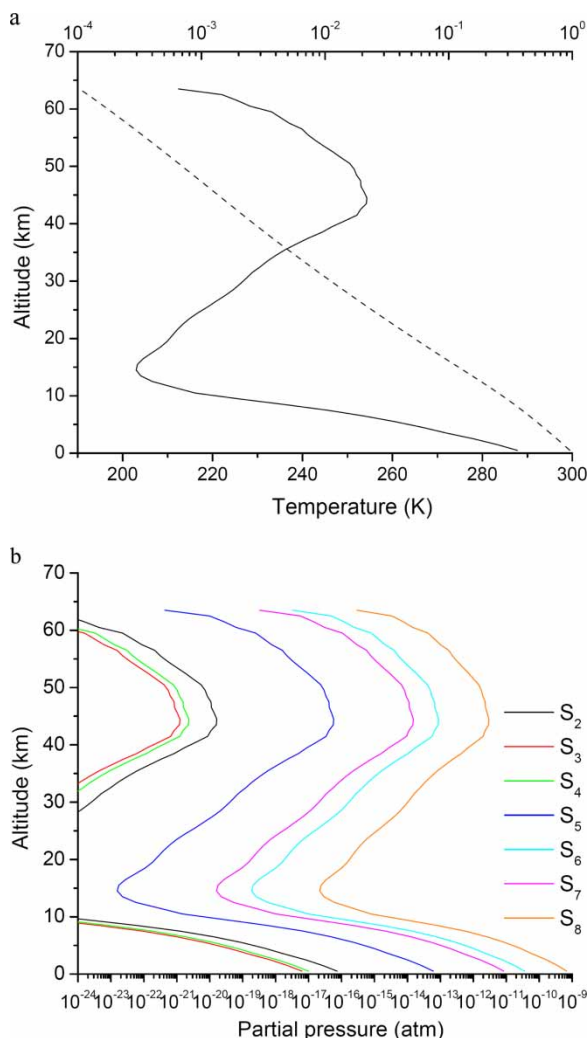


Figure 4. (a) Typical temperature and pressure (upper scale, in atmospheres) versus altitude profiles for the modern Earth atmosphere. (b) Predicted equilibrium vapor pressures for sulfur allotropes corresponding to the temperature profile in (a). Vapor pressures are computed for a background gas pressure of 1 atm at all altitudes.

4. Discussion

The low sulfur allotrope vapor pressures shown in Figure 3 have implications for early Earth atmospheric chemistry models and the formation mechanism of S-MIF for the interpretation of S_2 observed at the comet Shoemaker-Levy 9 impact sites on Jupiter, for sulfur allotropes in the atmosphere of Venus, and for the temperatures of volcanic plumes on Io. As an example of early Earth atmospheric models, Kasting (27) computed S_2 partial pressure $\sim 10^{-12}$ atm for a surface temperature of 280 K, which is five orders of magnitude above the saturation pressure estimated here (Figure 3). Equilibrium S_2 partial pressure $\sim 10^{-12}$ is consistent with a surface temperature ~ 340 K and is closer to the surface temperature assumed in Kasting *et al.* (1). In these models, S_8 is formed through a series of gas phase association reactions including



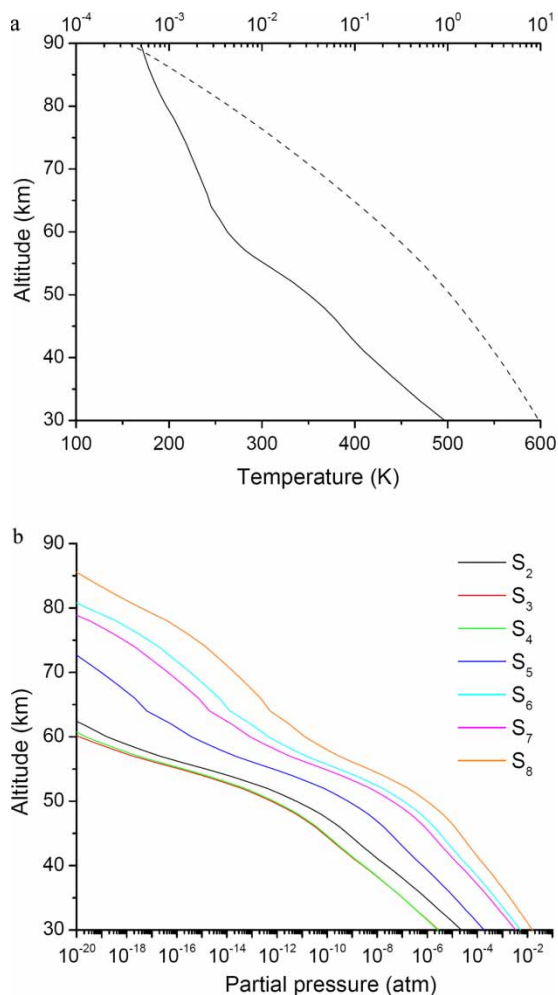


Figure 5. (a) Temperature and pressure (upper scale, in atmospheres) versus altitude from 30 to 90 km in the atmosphere of Venus (26). (b) Predicted equilibrium vapor pressures for sulfur allotropes corresponding to the temperature profile in (a). Below 30 km in the Venus atmosphere, additional thermochemical reactions become important. Vapor pressures are computed for a background gas pressure of 1 atm at all altitudes.

and followed by reactions (3a) and (3b). For lower temperature atmospheres (<300 K), S_2 , S_3 , and S_4 will condense out, most likely onto the surfaces of existing atmospheric particles, which may interfere with reactions (3a) and (3b). Because sulfur polymerization can continue in the solid phase, the net result may be to form S_8 on the surface of particles rather than in the gas phase, which may mean that the photochemical model results are only slightly affected. Full atmospheric modeling with condensation reactions needs to be done to address this point.

The origin of the S-MIF measured in ancient sedimentary rocks is still debated. Laboratory experiments (28) and radiative transfer calculations (12) suggest that SO_2 photodissociation in the atmosphere could be the source. However, by analogy with oxygen MIF produced during O_3 formation (6), which is attributed to a symmetry-dependent non-statistical redistribution of internal energy in the vibrationally excited O_3 (7), it is possible that reactions such as $S + S_2 \xrightarrow{M} S_3$ and $S_2 + S_2 \xrightarrow{M} S_4$ also produce MIF signatures. The low vapor pressures of S_2 , S_3 , and S_4 for expected atmospheric temperatures suggest that it is unlikely that S_3 and S_4 formed in the gas

phase in the Archean atmosphere. However, the loss rates of these species must be considered. This will be discussed further below for the atmosphere of Venus using known particle number densities. For the Archean Earth, I will simply point out that for an S_2 mixing ratio of 10^{-12} , the timescale for loss of S_2 by reaction (3a) is ~ 100 s in the troposphere using the fastest published rate constant (29). A reliable condensation timescale is impossible to determine for the Archean troposphere, but using modern troposphere values of particle diameter $\sim 0.2 \mu$ and particle number density $\sim 1000 \text{ cm}^{-3}$ (30) yields a condensation timescale ~ 100 s, comparable to the S_2 loss timescale due to gas phase formation of S_4 . This suggests that although S_2 is highly supersaturated, gas phase formation of S_3 and S_4 may still occur, and may therefore be the sources of S-MIF in the atmosphere. This conclusion is dependent on the very uncertain rate coefficient for reaction (3a). If the rate constant for Equation (3a) is much lower than published values (29), then S_2 would condense out and form S_3 , S_4 , and other allotropes on particle surfaces. Ozone formed on surfaces (*e.g.* on the walls of a reaction vessel) does not exhibit a MIF signature (31), which argues against the formation of S-MIF during solid-phase reactions among sulfur allotropes.

If the surface and atmosphere of the Earth were much warmer than today, as has been suggested based on oxygen isotopes in Archean cherts (*e.g.* ref. (32, references therein)), higher allotrope vapor pressures would have been allowed. For example, a surface temperature of 70°C (32) would imply S_2 and S_3 saturated number densities of 10^7 and 10^6 cm^{-3} , which would facilitate gas phase formation of S_3 and S_4 . Such high surface and ocean temperatures, although suggested by the chert data, are very difficult to account for in climate models given that solar luminosity during the Archean was only about 70% of the modern value.

Sulfur is a well-known constituent of the Venus atmosphere. At cloud heights, most sulfur is in the form of sulfuric acid aerosols formed by upwelling SO_2 and H_2O . When the abundance of O_2 (a photochemical product of CO_2 and H_2O photolysis) is low, SO_2 is photolyzed and the sulfur can undergo a net disproportionation (33)



Sulfur atoms recombine to form heavier allotropes and elemental sulfur aerosols, which together with sulfuric acid aerosols, descend into the lower atmosphere and are converted to OCS at high temperatures (13). The aerosol mass ratio of $\text{S}_8/\text{H}_2\text{SO}_4$ was observed to be ~ 0.1 in the upper levels of the clouds (34). Atmospheric absorption in the upper cloud deck (~ 60 km) at wavelengths below 320 nm is accounted for by SO_2 , but an additional absorber at short visible wavelengths imparts a slight yellowish colour to Venus. The two leading hypotheses for the absorber are: (1) the condensed sulfur allotropes S_3 and S_4 present at a mass fraction of a few percent in S_8 particles (14); and (2) $\sim 1\%$ FeCl_3 in a sulfuric acid solution (the FeCl_3 is proposed to be derived from surface rocks and transported upward by eddy motions) (35). I will not consider FeCl_3 here, but will estimate the condensation timescale for the low-mass sulfur allotropes (S_2 , S_3 , S_4) in the upper Venus cloud deck, because they are rapidly dissociated in the gas phase.

In the free molecule regime, the rate of condensation onto particles is given by the quantity $\alpha c S/4$, where α is the accommodation coefficient, $c = \sqrt{8kT/\pi m}$ is the thermal velocity of the gas, and $S = 4\pi a^2 N$ is the surface area density of particles for a particle radius a and particle number density N . Inverting the rate to obtain a timescale, the condensation timescale may then be defined as

$$t_c = \frac{1}{\alpha c \pi a^2 N}. \quad (7)$$

The upper cloud deck of Venus has $N \sim 300 \text{ cm}^{-3}$ and $a \sim 1.5 \mu$, which for S_2 at temperature of 250 K yields $t_c \sim 2$ s, assuming an accommodation coefficient of unity. Photochemical models (36) estimate the photolysis rate coefficient of S_2 to be 0.012 s^{-1} in the Venus upper atmosphere. Thus, condensation of S_2 will be more rapid than photolysis, assuming $\alpha > 10^{-2}$ for sticking of

S_2 onto sulfuric acid particles. Note that the free molecule regime is valid for Knudsen number $Kn = \lambda/a \gg 1$, where λ is the mean-free path in the gas. At 60 km in the Venus atmosphere, $\lambda \sim 0.4 \mu$, so $Kn \sim 2.7$, which suggests that Knudsen flow is probably important, although I will neglect it here.

Gas phase formation of S_3 and S_4 requires a substantial S_2 mixing ratio. The most recent measured rate constant for S_4 formation by Reaction (3a) is $2.2 \times 10^{-29} \text{ cm}^6 \text{ s}^{-1}$ (29). At 60 km, formation of S_4 will occur more rapidly than S_2 condensation for an S_2 mixing ratio >1 ppb. Given that S_2 has not been observed in the Venus atmosphere, this may be an unrealistically high value. Gas phase S_3 and S_4 are photolyzed at visible wavelengths on timescales of $\ll 10^2$ s, and therefore have less opportunity to undergo condensation. From the above considerations, it seems most likely that S_3 and S_4 form via heterogeneous reactions on sulfuric acid particles rather than via gas phase reactions. Conversion of condensed lighter allotropes to S_8 occurs on a timescale consistent with the disappearance of UV features in the Venus atmosphere (14).

Abundant S_2 was observed at one of the impact sites (site G) of the fragments of comet Shoemaker-Levy 9 with Jupiter (15). Modeling of absorption by S_2 in bands 5–0 to 9–0 of the B–X system and at a temperature of 300 K yielded a column density $\sim 3 \times 10^{18} \text{ cm}^{-2}$ in the observing aperture of the faint object spectrograph (FOS) on the Hubble space telescope (HST). Consideration of the observing aperture and S_2 line saturation suggested that $\sim 10^{14}$ g of S_2 were present in the Jovian atmosphere (15). The observation at site G was made 3 h after impact of the G fragment. S_2 was again observed at site G 3.5 days after impact, but was not detected 3 weeks later. It has been determined that S_2 in the Jovian stratosphere is destroyed by photolysis on a timescale of $\sim 2 \times 10^4$ s (17). Furthermore, the detection of S_2 at site G 3.5 days after impact may have been S_2 at the nearby S impact site ('S' refers to an impacting comet fragment and not to atomic sulfur) formed only 45 min before the second G site observation was made (17).

Modeling work assumes a volume mixing ratio for S_2 of 10^{-6} at a pressure of 10^{-3} atm. The unperturbed (by an impact) atmospheric temperature on Jupiter at 10^{-3} atm is $\sim 170 - 200$ K. Even at an elevated temperature of 300 K, the equilibrium vapor pressure for S_2 is $\sim 10^{-15}$ atm, implying that for the conditions assumed by Noll *et al.* (15), S_2 is supersaturated by a factor of 10^6 . The S_2 loss timescale due to Reaction (3a) is ~ 100 s. Massive brown features were left at each impact site with dark central cores and lighter distal material. The cores were comprised of particles with radius $\sim 0.1 \mu$ and number density $\sim 600 \text{ cm}^{-3}$ (37), implying an S_2 condensation timescale ~ 200 s; longer condensation times would apply in the distal regions of the impact features. Thus, loss of S_2 at the impact sites occurred by both gas phase formation of S_3 and S_4 , as modeled in ref. (9), and by condensation of the highly supersaturated S_2 vapor. The observation of S_2 at the G impact site about 3 h after impact is consistent with the S_2 photolysis timescale, but indicates that the loss timescales for both Reaction (3a) and condensation are too short. This could result from rapid photolysis of S_4 , which would recycle S_2 ; from an accommodation coefficient $\ll 1$; and from S_2 primarily in the distal portions of the impact feature. Another alternative, suggested in ref. (16, Abstract), is that the S_2 absorption spectra observed by HST are better fit by S_2 gas at much higher temperatures (~ 1200 K). This would imply that the S_2 was in the Jovian thermosphere (pressures $< 10^{-6}$ atm), at altitudes well above most of the other post impact molecular detections. The lower pressures would remove concerns about rapid loss due to Reaction (3a), and the higher temperature would ensure that gas phase sulfur allotropes remain subsaturated. However, this argument is better made on the basis of high temperature absorption spectra for S_2 .

Finally, S_2 has also been observed in volcanic plumes in the atmosphere of Io, the innermost Galilean satellite of Jupiter (18). S_2 was observed in absorption in the B–X band system against the Jovian atmosphere using the space telescope imaging spectrograph (STIS) instrument on HST from 240 to 310 nm. An S_2 column density of $\sim 1 \times 10^{16} \text{ cm}^{-2}$ and an S_2/SO_2 ratio ~ 0.1 were inferred. The latter value is consistent with equilibrium with silicate magma at temperatures ~ 1300 K (18). For the assumption of a uniform density and temperature plume, the rotational

temperature of S_2 was inferred to be between 300 and 500 K. For an observed plume height of 350 km, the S_2 gas pressure is $\sim 10^{-11}$ atm. The equilibrium vapor pressure of S_2 is $\sim 10^{-15}$ atm at 300 K (Figure 3) and $\sim 10^{-5}$ atm at 500 K (Figure 2), suggesting that S_2 would be strongly supersaturated if the plume temperature is ~ 300 K. I again compare timescales for several processes involving S_2 in the plume. The plume dynamical (ballistic trajectory) timescale is ~ 24 min (18). The S_2 photolysis timescale is ~ 3 h at Jupiter. In model calculations (38), the S_2 loss timescale due to Reaction (3a) is $\sim 5 \times 10^7$ s near the base of a plume with number density $\sim 10^{11}$ cm^{-3} (density from ref. (38)). To compute the condensation timescale, an estimate of the dust particle size and abundance in the plume is needed. From absorption measurements, a particle diameter of 0.08μ and a total plume dust mass $\sim 1.2 \times 10^9$ g have been determined (39). For a plume scale height of ~ 50 km, and a plume diameter comparable to the plume height (400 km), the number density of particles is ~ 400 cm^{-3} . The S_2 condensation timescale is 2700 s, which is comparable to the plume dynamical timescale. Thus, condensation reactions for all allotropes are likely to be important and should be included in chemical models, which at present only include S_8 condensation (8). Condensation of S_2 on grains and further polymerization to S_3 and S_4 on the grain surfaces likely contributes to the orange-red colouration on the surface of Io near the plume base.

5. Conclusions

The low vapor pressure of sulfur vapor over solid sulfur together with equilibrium vapor pressures of sulfur allotropes over liquid sulfur scaled to lower temperatures argues that the equilibrium vapor pressures of low mass allotropes (*i.e.* S_2 , S_3 , S_4) over solid sulfur must be very low. At typical atmospheric temperatures, the abundances of sulfur allotropes in the ancient Earth atmosphere would have been far lower than previously estimated. This would appear to argue against gas phase reactions among low mass allotropes as the mechanism for S-MIF observed in ancient sulfur-bearing rocks. However, the kinetics of condensation and gas-phase polymerization reactions may allow for gas phase formation of S_3 and S_4 from S and S_2 , even though S_2 would be supersaturated by many orders of magnitude. This implies that reactions such as $S + S_2 \xrightarrow{M} S_3$ and $S_2 + S_2 \xrightarrow{M} S_4$ may be sources of S-MIF in the primitive atmosphere. In the upper cloud deck of Venus photolytic disproportionation of SO_2 (for locally low O_2) can produce S_2 . Condensation of S_2 onto sulfur and/or sulfuric acid cloud particles is likely to be the fastest process, assuming an accommodation coefficient near unity. This implies that if the blue absorber in the upper cloud deck is in fact due to S_3 and S_4 in cloud particles, the S_3 and S_4 most likely formed by polymerization reactions on the particle surface, rather than in gas-phase reactions. In this case, photolysis of S_3 and S_4 (34) is not relevant. At the G impact site of comet Shoemaker-Levy 9 with Jupiter, the observation of absorption by gas-phase S_2 3 h after impact implies photochemical recycling of S_2 and slower condensation timescales than the assumption of a unity accommodation coefficient would suggest. The possibility that the S_2 was in the Jovian thermosphere at high temperatures (~ 1200 K) is not constrained by considerations of sulfur allotrope vapor pressures. The dust and S_2 content of volcanic plumes on Io suggest that S_2 condensation should be important on the dynamical timescale of the plume. Further polymerization of sulfur allotropes on dust particles will produce S_3 and S_4 , which would contribute to the coloration of the surface of the Io near the volcanic source.

These conclusions are weakened by many uncertainties. The rate coefficient data for gas phase sulfur allotrope reactions are often based on fits to reactions mechanisms, and is therefore very difficult to evaluate. Direct measurements or high quality *ab initio* results are needed. The lack of data on accommodation coefficients for sulfur allotrope heterogeneous reactions with sulfuric acid and other particles also greatly limits the interpretations presented here. Consideration of

the role of other condensation nuclei in condensation of highly supersaturated sulfur allotrope species is also needed, and will be discussed elsewhere.

Acknowledgements

The author thanks K. Zahnle and an anonymous referee for helpful reviews, and gratefully acknowledges support from the UCLA IGPP Center for Astrobiology and the NASA Astrobiology Institute, and from the NASA Exobiology and Evolutionary Biology Program (Grant No. NNX07AK63G).

References

- (1) Kasting, J.F.; Zahnle, K.J.; Pinto, J.P.; Young, A.T. *Orig. Life Evol. Biosph.* **1989**, *19*, 95.
- (2) Pavlov, A.; Kasting, J. *Astrobiology* **2002**, *2*, 27.
- (3) Zahnle, K.; Claire, M.; Catling, D. *Geobiology* **2006**, *4*, 271.
- (4) Farquhar, J.; Bao, H.; Thiemens, M. *Science* **2000**, *289*, 756.
- (5) Clayton, R.N. *Ann. Rev. Earth Planet Sci.* **1993**, *21*, 115.
- (6) Thiemens, M.H. *Science* **1999**, *283*, 341.
- (7) Gao, Y.Q. and Marcus, R.A. *Science* **2001**, *293*, 259.
- (8) Clayton, R.N. *Nature* **2002**, *415*, 860.
- (9) Yurimoto, H.; Kuramoto, K. *Science* **2004**, *305*, 1763.
- (10) Lyons, J.R.; Young, E.D. *Nature* **2005**, *435*, 317.
- (11) Marcus, R.A. *J. Chem. Phys.* **2004**, *121*, 8201.
- (12) Lyons, J.R. *Geophys. Res. Lett.* **2007**, *34*, L22811.
- (13) Krasnopolsky, V.A.; Pollack, J.B. *Icarus* **1994**, *109*, 58.
- (14) Toon, O.B.; Turco, R.P.; Pollack, J.B. *Icarus* **1982**, *51*, 358.
- (15) Noll, K.S. *et al. Science* **1995**, *267*, 1307.
- (16) Yelle, R.V.; McGrath, M.A. *Bull. Amer. Astron. Soc.* **1995**, *27*, 1118.
- (17) Moses, J.I. In *The Collision of Comet Shoemaker-Levy 9 and Jupiter*; Noll, K.S., Weaver, H.A., Feldman, P.D., Eds.; Cambridge University Press: Cambridge, UK, 1996; pp 243–268.
- (18) Spencer, J.R.; Jessup, K.L.; McGrath, M.A.; Ballester, G.E.; Yelle, R. *Science* **2000**, *288*, 1208.
- (19) Peng, D.-Y.; Zhao, J. *J. Chem. Thermodynam.* **2001**, *33*, 1121.
- (20) Foutetier, G. *Comput. Rend.* **1944**, *218*, 194.
- (21) Neumann, K. *Z. Phys. Chem.* **1934**, *A171*, 416.
- (22) Rau, H.; Kutty, T.R.N.; Guedes de Carvalho, J.R.F. *J. Chem. Thermodynam.* **1973**, *5*, 833.
- (23) Detry, D.; Drowart, J.; Goldfinger, P.; Keller, H.; Rickert, H. *Z. Phys. Chem. N. F.* **1967**, *55*, 314.
- (24) Elbanowski, M. *Roczniki Chemii Ann. Soc. Chim. Polonorum* **1969**, *43*, 1883.
- (25) Elbanowski, M. *Roczniki Chemii Ann. Soc. Chim. Polonorum* **1970**, *44*, 801.
- (26) Seiff, A.; Schofield, J.T.; Kliore, A.J.; Taylor, F.W.; Limaye, S.S.; Revercomb, H.E.; Sromovsky, L.A.; Kerzhanovich, V.V.; Moroz, V.I.; Marov, M.Y. *Adv. Space Res.* **1985**, *5*, 3.
- (27) Kasting, J.F. *Orig. Life Evol. Biosph.* **1990**, *20*, 199.
- (28) Farquhar, J.; Savarino, J.; Airieau, S.; Thiemens, M.H. *J. Geophys. Res.* **2001**, *106*, 32829.
- (29) Nicholas, J.E.; Amodio, C.A.; Baker, M.J. *J. Chem. Soc. Faraday Trans. 1* **1979**, *75*, 1868.
- (30) Schmeling, M. *et al. Tellus* **2000**, *52B*, 185.
- (31) Mauersberger, K.; Krankowsky, D.; Janssen, C.; Schinke, R. *Adv. Atom. Mol. Opt. Phys.* **2005**, *50*, 1.
- (32) Knauth, L.P.; Lowe, D.R. *Geol. Soc. Am. Bull.* **2003**, *115*, 566.
- (33) Esposito, L.W.; Bertaux, J.-L.; Krasnopolsky, V.; Moroz, V.I.; Zazova, L.V. In *Venus II*; Bougher, S.W., Hunten, D.M., Phillips, R.J., Eds.; University of Arizona Press: Tucson, AZ; pp 415–458.
- (34) Krasnopolsky, V.A. *Planet Space Sci.* **2006**, *54*, 1352.
- (35) Zasova, L.V.; Krasnopolsky, V.A.; Moroz, V.I. *Adv. Space Res.* **1981**, *1*, 13.
- (36) Mills, F.P.; Allen, M. *Planet Space Sci.* **2007**, *55*, 1729.
- (37) West, R.A. In *The Collision of Comet Shoemaker-Levy 9 and Jupiter*; Noll, K.S., Weaver, H.A., Feldman, P.D., Eds.; Cambridge University Press: Cambridge, UK, 1996; pp 269–292.
- (38) Moses, J.I.; Zolotov, M.Yu.; Fegley, B. *Icarus* **2002**, *156*, 76.
- (39) Spencer, J.R. *et al. Geophys. Res. Lett.* **1997**, *24*, 2471.
- (40) Meyer, B. *Chem. Rev.* **1976**, *76*, 367.
- (41) Sander, U.H.F.; Fischer, H.; Rothe, U.; Kola, R. *Sulphur, Sulphur Dioxide and Sulphuric Acid*; The British Sulphur Corp.: London, UK, 1984; p 12.